NJC

Accepted Manuscript



Journal Name

View Article Online
DOI: 10.1039/C8NJ05796F

ARTICLE

# Supramolecular phenoxy-alkyl maleate based hydrogels and its enzyme/pH responsive curcumin release

Received 00th January 20xx,
Accepted 00th January 20xx

DOI: 10.1039/x0xx00000x

www.rsc.org/

Bijari Anil Kumar[ab], Rati Ranjan Nayak*[ab]

Low-molecular-weight gelators that self-assemble via non-covalent interactions have been attracted considerable attention due to their good biocompatibility, low toxicity, inherent biodegradability as well as their convenience of design. Enzymatically digestible and pH sensitive hydrogels play an important role in controlled drug delivery applications. In the present study, we have synthesized four simple phenoxy alkyl maleate amphiphiles at various hydrophobic chain lengths ($C_6$-$C_{12}$). Gelation ability of four amphiphiles was examined in phosphate buffer solution, among them, the maleates with $C_{10}$ and $C_{12}$ chain lengths exhibited gelation ability at the minimum gelation concentration (MGC) of 1.6 and 1.3% w/v respectively. This hydrogelators has shown strong three-dimensional cross-linked networks, which can capture water molecules. Obtained supramolecular hydrogels were thoroughly characterized by using differential scanning calorimetry (DSC), scanning electron microscopy, density functional theory (DFT) calculation, X-ray diffraction, and rheological studies. More importantly, curcumin, the hydrophobic drug has been encapsulated (1% w/v) into the gel core and subsequent release has been achieved through gel-to-sol transition induced by lipozyme (biological stimuli). Additionally the drug loaded hydrogel exhibited pH response drug release behavior. The drug release behavior was monitored by employing UV-vis spectroscopy. Overall, the prepared hydrogelators may useful to stimuli responsive delivery of hydrophobic drugs.

## Introduction

Hydrogels are capable of trapping a large amount of water without being dissolved and also constructions of three-dimensional network structure. The hydrogen bonds, π-π stacking, van der Waals forces, and other interactions are useful in construction of network structures inside the hydrogel.[1–6] Depending on methods of preparation, hydrogels can be classified into physically cross-linked hydrogels and chemically cross-linked hydrogels. Physical cross-linking relies on molecular interactions for the maintenance of network integrity, thus can be made reversible or responsive to changes in temperature and pH.[7–9] Strong hydrogelation ability in phosphate-buffered saline solution a biological medium was reported by Gao and Tan groups.[10–11] The hydrogels have been widely used in various kinds of applications, particularly in the biomedical fields such as tissue engineering, wound healing, and drug delivery.[12–14]

The hydrogels formed by either macromolecules or low molecular weight molecules gained immense interest in recent years.[15–18] From past two decades, low-molecular weight hydrogelators (LMWHGs) gain considerable interest, because of their advantages of being easily designed with good biodegradability causing less side-effect. The low-molecular weight hydrogels have many advantages in novel drug delivery systems. Primarily, they have high drug loading capacity than normal delivery systems. Secondly, encapsulation of drugs into the hydrogel or formation of the hydrogel by a drug derivative itself can eliminate the unexpected side effects from inactive substances. The design of the LMWHGs with an enzyme sensitive functionality has the most important advantage for controlled and sustained release of drugs. These all features put forward the huge potential of low-molecular weight hydrogels for the delivery of drugs. The highly porous structures of hydrogels enables the drug loading in gel interior network structures and allows subsequent slow and persistent drug release at a rate dependent on the diffusion co-efficient of the gelator molecule from the gel networks.[19] Most of the pharmaceutical drugs (nearly 70%) are poorly soluble in water, it leads to low oral bioavailability. However, hydrogels are useful for improving solubility and bioactivity of hydrophobic drug in vitro study.[20] Hydrophobic drug like turmeric (Curcuma longa rhizomes) have wide variety of pharmacological properties such as anti-oxidant, anti-inflammatory, anti-bacterial, and anti-tumor activities.[21–24] Old generation peoples used curcumin in traditional ayurvedic formulations for the treatment of various types of skin infections.[25]

[a]Centre for Lipid Science and Technology, CSIR-Indian Institute of Chemical Technology, Hyderabad-500 007, India
[b]Academy of Scientific and Innovative Research, New Delhi-110 025, India
E-mail address: rrnayak@iict.res.in Ph: +91-40-27191838, Fax: +91-40-27193370
Electronic Supplementary Information (ESI) available: See DOI: 10.1039/x0xx00000x

View Article Online
DOI: 10.1039/C9NJ05796F



The drug release from the drug loaded hydrogel can be controlled by modifying the gel network structure in response to external stimuli. For example, external stimuli like pH, temperature, and enzymes were mentioned as main factors for the release of loaded drug in hydrogels at appropriate time with site of action.[25–29] In living organisms, most of the biology processes are controlled by enzymes. Zelzer et al. used enzyme responsive materials for controlled drug delivery.[30] Various types of enzymes like amylase, trypsin, and lipase were used for the investigation of drug delivery process through enzymatic degradation of the drug-loaded hydrogels.[29,31–32] Takeda et al. prepared hydrogels with potential medical use in phosphate buffer and subsequent gel degradation by lysozyme.[33] Herein enzyme is involved in specific degradation of the gel network structure, it leads to the drug release from the drug-loaded hydrogel.

The present article deals with phenoxy-alkyl maleates based amphiphiles which might be helpful in the formation of hydrogels with non-covalent interactions. The synthesized molecules are tested for their hydrogelation ability in this report. The various functional groups present in the amphiphiles such as, aromatic group may useful form π-π stacking, alkyl group may involve in van der Waals forces, and maleate group may participate in hydrogen bonding.[34–35] All these interactions may joined together for the formation of stable hydrogel networks. This type of gels may be useful to entrap the chemotherapeutic hydrophobic drug. Furthermore, the entrapped drug may be released by the specific enzyme as well as at acidic pH. The drug encapsulation and release study of phenoxy-alkyl maleates based hydrogels using curcumin, a model anticancer agent was reported in this article.

## Experimental section

### Materials

Phenol, maleic anhydride, and the analytical grade solvents were purchased from SRL, Mumbai, India. 12-Bromo-1-dodecanol, 10-bromo-1-decanol, 8-bromo-1-octanol, 6-bromo-1-hexanol, and curcumin were purchased from Sigma Aldrich, USA. Lypozyme was purchased from novozymes, Denmark. If necessary for purification, distillation was done for solvents.

### Methods

$^1$H and $^{13}$C NMR spectra of synthesized molecules in $CDCl_3$ solvent were recorded on AVANCE-500 (Bruker), a 500 MHz NMR spectrometer. Chemical shifts values were measured in ppm with reference to TMS. The molecular mass of the synthesized compounds were identified by ESI–MS and HRMS. The UV–vis absorption spectra were obtained with a Perkin Elmer (model Lambda 35) spectrophotometer.

### General procedure for phenoxy-alkanol (n-PA) synthesis

The William ether synthesis was performed as shown in Scheme 1, n-bromo-alcohol (0.0265 mol) was added to the mixture of phenol (2.5 g; 0.0265 mol), $K_2CO_3$ (14.6 g; 0.1060 mol), and a catalytic amount of KI (0.8 g; 0.0053 mol) in

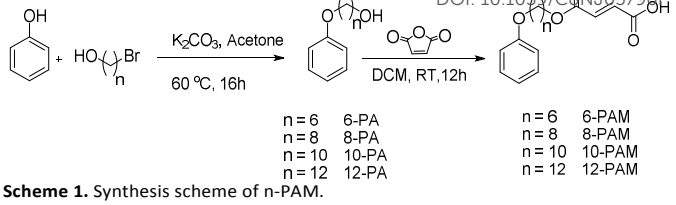


**Scheme 1.** Synthesis scheme of n-PAM.

acetone and refluxed for 16h. Acetone was removed in a rotary evaporator after completion of the reaction. The obtained crude mixture was diluted with ethyl acetate and washed with brine solution. The organic layer was dehydrated over anhydrous sodium sulphate. Volatiles were removed through vacuum and purified by column chromatography using chloroform.

***6-Phenoxyhexan-1-ol (6-PA)***

Liquid, yield: 75%. $^1$H NMR (500 MHz, $CDCl_3$): δ ppm, 7.23–7.32 (m, 2H, HAr), 6.85–6.97 (m, 3H, HAr), 3.94 (t, *J* = 6.6 Hz, 2H, –$OCH_2$– ), 3.63 (t, *J* = 6.6 Hz, 2H, –$OCH_2$–), 1.72–1.82 (m, 2H, –$CH_2$–), 1.51–1.63 (m, 2H, –$CH_2$–), 1.28–1.51 (m, 4H, –$(CH_2)_2$–), ESI–MS *m/z* calculated for $C_{12}H_{19}O_2$ $[M + H]^+$ 195.14, found 195.16.

**8-Phenoxyoctan-1-ol (8-PA)**

White solid, yield: 78%. $^1$H NMR (500 MHz, $CDCl_3$) δ ppm, 7.23–7.30 (m, 2H, HAr), 6.85–6.95 (m, 3H, HAr), 3.93 (t, *J* = 6.6 Hz, 2H, –$OCH_2$–), 3.61 (t, *J* = 6.6 Hz, 2H, –$OCH_2$–), 1.72–1.82 (m, 2H, –$CH_2$–), 1.51–1.60 (m, 2H, –$CH_2$–), 1.40–1.50 (m, 2H, –$CH_2$– ), 1.29–1.40 (m, 6H, –$(CH_2)_3$–). ESI–MS *m/z* calculated for $C_{14}H_{22}NaO_2$ $[M + Na]^+$ 245.15, found 245.34.

**10-Phenoxydecan-1-ol (10-PA)**

White solid, yield: 82%. $^1$H NMR (500 MHz, $CDCl_3$) δ ppm, 7.22–7.32 (m, 2H, HAr), 6.86–6.97 (m, 3H, HAr), 3.94 (t, *J* = 6.6 Hz, 2H, –$OCH_2$–), 3.62 (t, *J* = 6.6 Hz, 2H, –$OCH_2$–), 1.71–1.82 (m, 2H, –$CH_2$–), 1.51–1.61 (m, 2H, –$CH_2$–), 1.40–1.50 (m, 2H, –$CH_2$– ), 1.23–1.39 (m, 10H, –$(CH_2)_5$–), ESI–MS *m/z* calculated for $C_{16}H_{26}NaO_2$ $[M + Na]^+$ 273.18, found 273.17.

***12-Phenoxydodecan-1-ol (12-PA)***

White solid, yield: 82%. $^1$H NMR (500 MHz, $CDCl_3$) δ ppm, 7.22–7.32 (m, 2H, HAr), 6.86–6.97 (m, 3H, HAr), 3.94 (t, *J* = 6.5 Hz, 2H, –$OCH_2$–), 3.63 (t, *J* = 6.5 Hz, 2H, –$OCH_2$–), 1.73–1.81 (m, 2H, –$CH_2$–), 1.52–1.60 (m, 2H, –$CH_2$–), 1.40–1.49 (m, 2H, –$CH_2$– ), 1.24-1.39 (m, 14H, –$(CH_2)_7$–), ESI–MS *m/z* calculated for $C_{18}H_{30}NaO_2$ $[M + Na]^+$ 301.21, found 301.03.

### General procedure for n-PAM synthesis

A mixture of n-PA and maleic anhydride (1:1 mol ratio) were stirred in dichloromethane for 12h. The crude product obtained after solvent evaporation and column chromatography was used for the purification (ethyl acetate (2): hexane (8)). Further, the product was recrystallized using chloroform and hexane (1:1) solvent system.

View Article Online
DOI: 10.1039/C8NJ05705F



**4-Oxo-4-((6-phenoxyhexyl)oxy)but-2-enoic acid (6-PAM)**

White solid, yield: 82%. $^1$H NMR (500 MHz, $CDCl_3$) δ ppm, 7.24–7.31 (m, 2H, HAr), 6.87–6.96 (m, 3H, HAr), 6.40 (d, *J* = 12.8 Hz, 1H, –CH=), 6.36 (d, *J* = 12.8 Hz, 1H, –CH=), 4.27 (t, *J* = 6.7 Hz, 2H, $–OCH_2–$), 3.95 (t, *J* = 6.5 Hz, 2H, $–OCH_2–$), 1.67–1.82 (m, 4H, $–CH_2–$), 1.32–1.52 (m, 4H, $–(CH_2)_2–$). $^{13}$C NMR (500 MHz, $CDCl_3$) δ ppm, 167.82, 164.14, 158.88, 136.42, 129.59, 120.64, 114.50, 67.67, 63.11, 29.09, 28.03, 25.75. HRMS *m/z* calculated for $C_{16}H_{19}O_5$ $[M–H]^–$ 291.1238, found 291.1233.

**4-Oxo-4-((8-phenoxyoctyl)oxy)but-2-enoic acid (8-PAM)**

White solid, yield: 85%. $^1$H NMR (500 MHz, $CDCl_3$) δ ppm, 7.24–7.31 (m, 2H, HAr), 6.86–6.97 (m, 3H, HAr), 6.44 (d, *J* = 12.6 Hz, 1H, –CH=), 6.36 (d, *J* = 12.8 Hz, 1H, –CH=), 4.27 (t, *J* = 6.7 Hz, 2H, $–OCH_2–$), 3.95 (t, *J* = 6.4 Hz, 2H, $–OCH_2–$), 1.68–1.83 (m, 4H, $–CH_2–$), 1.32–1.52 (m, 8H, $–(CH_2)_4–$), $^{13}$C NMR (500 MHz, $CDCl_3$) δ ppm, 167.74, 164.66, 159.15, 136.04, 129.46, 120.33, 114.42, 67.81, 67.28, 29.17, 29.12, 28.99, 28.12, 25.89, 25.63. HRMS *m/z* calculated for $C_{18}H_{23}O_5$ $[M–H]^–$ 319.1551, found 319.1539.

**4-Oxo-4-((10-phenoxydecyl)oxy)but-2-enoic acid (10-PAM)**

White solid, yield: 88%. $^1$H NMR (500 MHz, $CDCl_3$) δ ppm, 7.24–7.31 (m, 2H, HAr), 6.86–6.96 (m, 3H, HAr), 6.44 (d, *J* = 12.7 Hz, 1H, –CH=), 6.37 (d, *J* = 12.7 Hz, 1H, –CH=), 4.27 (t, *J* = 6.7 Hz, 2H, $–OCH_2–$), 3.94 (t, *J* = 6.5 Hz, 2H, $–OCH_2–$), 1.65–1.84 (m, 4H, $–CH_2–$), 1.24–1.52 (m, 12H, $–(CH_2)_6–$). $^{13}$C NMR (500 MHz, $CDCl_3$) δ ppm, 167.78, 164.49, 159.05, 136.30, 129.38, 120.44, 114.44, 67.79, 67.22, 29.31, 29.01, 25.98, 25.67. HRMS *m/z* calculated for $C_{20}H_{27}O_5$ $[M–H]^–$ 347.1864, found 347.1851.

**4-Oxo-4-((12-phenoxydodecyl)oxy)but-2-enoic acid (12-PAM)**

White solid, yield: 86%. $^1$H NMR (500 MHz, $CDCl_3$) δ ppm, 7.23–7.32 (m, 2H, HAr), 6.86–6.97 (m, 3H, HAr), 6.44 (d, *J* = 12.8 Hz, 1H, –CH=), 6.36 (d, *J* = 12.8 Hz, 1H, –CH=), 4.27 (t, *J* = 6.7 Hz, 2H, $–OCH_2–$), 3.94 (t, *J* = 6.6 Hz, 2H, $–OCH_2–$), 1.67–1.83 (m, 4H, $–CH_2–$), 1.24–1.51 (m, 16H, $–(CH_2)_8–$). $^{13}$C NMR (500 MHz, $CDCl_3$) δ ppm, 167.77, 164.64, 159.03, 136.18, 129.34, 120.44, 114.44, 67.81, 67.22, 29.46, 29.38, 29.33, 29.24, 29.07, 26.01, 25.69. HRMS *m/z* calculated for $C_{22}H_{31}O_5$ $[M–H]^–$ 375.2177, found 375.2163.

**Gel preparation**

A given mass of the gelator and 1 mL of phosphate buffer solution (pH 6, 7, 8, and 9) were placed in a vial and then heated until complete dissolution of the gelator. Then the solution was spontaneously cooled to room temperature and allowed for 30 min at room temperature. The minimum gelation concentration (MGC) was determined by measuring the minimum amount of gelator required for the formation of a stable gel at room temperature. The "stable to inversion of a test tube" method was used to evaluate the gel state.

**Thermal stability**

Gel-to-sol phase transition temperatures ($T_{gel}$) were measured with a tube inversion method. The gel sample was taken in a sealed tube. The sample was kept in a temperature controlled water bath. The water bath was heated at a rate of 1 °C min$^{-1}$. The temperature at which the viscous gel dropped down was considered as $T_{gel}$. The $T_{gel}$ was also determined by using differential scanning calorimetry (DSC). The Perkin Elmer DSC 6000, equipped with a nitrogen gas intra cooling system was utilized in this study. The gel was hermetically sealed in an alumina pan, and an empty alumina pan is considered as reference. The thermograms were recorded at a heating rate of 1 °C min$^{-1}$.

**Rheological measurement**

All rheological tests were carried out at 25 °C through a rheometer (Bohlin Instruments C-VOR, UK) operating in the 20 mm parallel-plate configuration and at a 1 mm gap distance. The temperature was controlled by the water circulating thermostatic bath. Strain sweeps were performed over a strain range from 0.1 to 100% (ω = 1 Hz). The frequency sweep test was carried out over a frequency range from 0.1 to 100 Hz at constant strain of 1%. Each experiment was repeated at least three times.

**Field emission scanning electronic microscopy (FE-SEM)**

The hydrogel was placed on the stubs to make thin film and freeze dried under lyophilization. The morphology analysis of freeze-dried hydrogels (xerogel) was carried out with the JEOL JSM-7610F FE-SEM with semi-in-lens detector instrument (Japan).

**X- ray diffraction (XRD)**

The XRD measurement was carried out in an EMPYREAN, PANalytical, Netherland, X-ray Diffractometer using CuKα anode material and operating at a voltage of 45 kV and current of 30 mA. For this experiment air-dried gel sample on the pre-cleaned glass slide was used.

**Drug loading**

Curcumin was selected as a model drug molecule in this study. For loading curcumin molecule, certain amount of gelator was added to the phosphate buffer solution (pH 8) at their MGC and then heated to form a clear solution. Weighed amount curcumin was added to the clear gelator solution at 25 °C. The solution was mixed thoroughly and allowed for 30 min at 25 °C. The amount of curcumin was increase until the stable gel formation was noticed. The drug loading content was calculated by using the following equation.

$$Drug\ loading\ content\% = \frac{Weight\ of\ the\ drug\ in\ hydrogel}{Weight\ of\ the\ hydrogel} \times 100$$

**Drug release studies**

Drug release from the curcumin composite gel was examined in two different ways: (i) enzyme triggered drug release and (ii)

View Article Online
DOI: 10.1039/C8NJ05796F



pH-responsive drug release. In enzyme sensitive drug release process, 0.5 mL of water or enzymatic solution (100 U/mL) was added above the hydrogel or drug-loaded hydrogel (1 mL) in a vial. At certain time interval a minute quantity of aliquot solution was taken from the vial, diluted with distil-water and then absorption spectra were recorded to monitor the drug release behaviour.[36]

In pH stimuli-responsive method, for equilibrium purpose, the curcumin encapsulated gel was placed at room temperature (RT) for one hour. After that, drug composed gel was transferred into 1 mL quartz cuvette of path length 0.1 cm and left for 10 min at RT. 50 µL of acidic buffer solution was added to the hydrogel and then mixed homogeneously. The gel degradation pattern was monitored by measuring the absorbance at 600 nm in kinetic absorption study.

### Density functional theory

The ground-state geometry of **10-PAM** and **12-PAM** gelator molecules were optimized with the B3LYP theory level using a basis set 6-31G*.[37]

## Results and discussion

### Gelation behaviour

A stable self-standing hydrogelation ability of n-PAM compounds were studied in phosphate buffer at pH 6, 7, 8, and 9 by heating-cooling method. Gelation ability of the synthesized molecules in buffer solutions was tested by the "stable-to-inversion of the test tube" method. Among all the gelators, opaque gels were observed for **10-PAM** and **12-PAM** gelators as shown in Fig. 1. The **10-PAM** and **12-PAM** gelators were dissolved in basic solution (pH > 8) and precipitation was observed when pH < 8. The terminal carboxylic acid groups of gelator molecules play a vital role in the formation of self-assembled network structures inside the hydrogel. However, under similar condition, the short chain analogues (**6-PAM** and **8-PAM**) were unable to form gels. The results have been presented in Table 1. Further, the hydrogelation of **10-PAM** and **12-PAM** could be achieved even after several heating-cooling cycles and it is thermo-reversible in nature. The prepared hydrogels are stable for more than six months at room temperature.

The intermolecular interactions (non-polar and polar) were the main driving force for construction of stable 3D interactions in the gel formation. Similarly a fine balance between hydrophilicity and hydrophobicity of the gelator molecule is important for gel formation. Here, except the hydrocarbon chain length all the gelator molecules are structurally similar. In general, the gelation ability of the gelator was quantitatively calculated by determining MGC, which is defined as the minimum amount of gelator required to gel 1 mL of solvent at a given temperature. The **10-PAM** and **12-PAM** gelators are able to form stable gels and the MGC values are decreasing with increase in chain length. The increase in hydrophobicity of the gelator favoured the gelation at low MGC.

**Table 1.** Gelation properties of n-PAM amphiphiles in phosphate buffer solution (pH 8).

| Compounds | Behavior | MGC (mg/mL) | $T_{gel}$ (K) | |
|---|---|---|---|---|
| | | | Tube inversion method | DSC |
| **6-PAM** | S | – | – | – |
| **8-PAM** | E | – | – | – |
| **10-PAM** | G | 16 | 311 | 309 |
| **12-PAM** | G | 13 | 324 | 321 |

S: soluble; E: emulsion; G: gel


**Fig. 1.** Photograph of vials showing gelation of n-PAM in phosphate buffer solution (pH 8).

### Thermal stability of the hydrogels

Most of the supramolecular gels are formed with physically cross linked networks that undergo thermally reversible gel-to-sol transition. Inverted-tube method is one of the best methods for determination of hydrogel's thermal stability. In a comparative study, at 1.6% w/v of gelator, the gel-to-sol transition temperature ($T_{gel}$) of **10-PAM** and **12-PAM** gelators was measured. The $T_{gel}$ measured by tube inversion method of **10-PAM** and **12-PAM** gels were 311 and 324 K respectively. Further, these gels are exhibited thermo reversibility. The DSC experiment was performed to know the $T_{gel}$. Hydrogel thermal

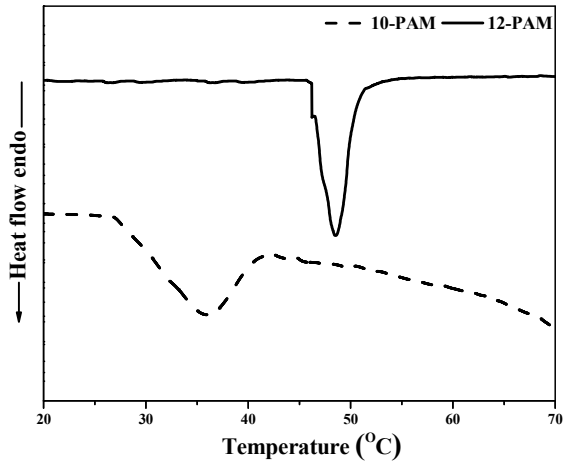


**Fig. 2.** Calorimetric curves of hydrogels.

View Article Online
DOI: 10.1039/C8NJ05796E



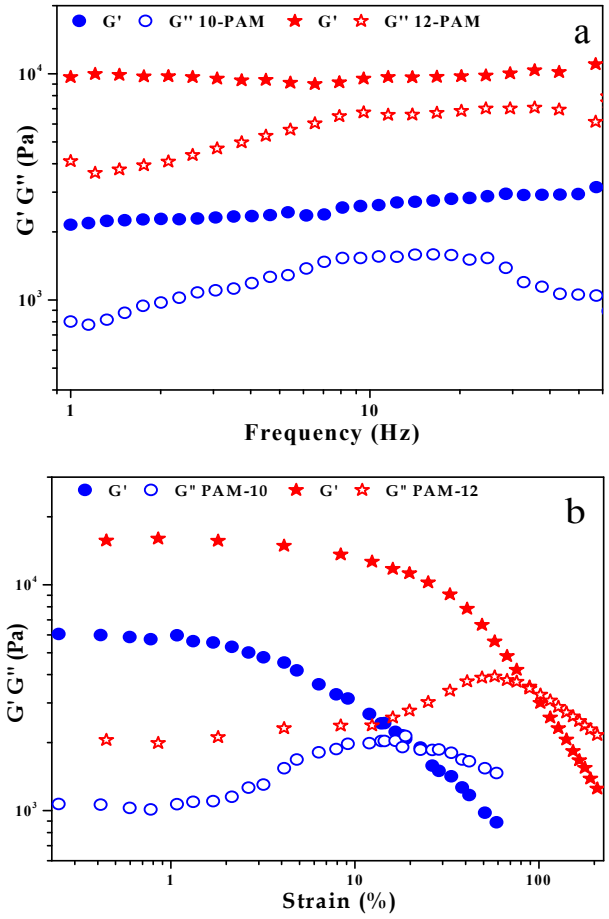


**Fig. 3**. (a) Dynamic frequency sweep rheological experiments for **10-PAM** (1.6 wt%) and **12-PAM** (1.6 wt%) at constant strain of 1%. (b) Dynamic strain amplitude rheological experiment for 10-PAM (1.6 wt%) and 12-PAM (1.6 wt%) at constant frequency 1 Hz.

stability results of tube inversion method was further supported by the DSC experiment (Table 1). From the DSC thermogram, similar results were observed as observed in tube inversion method within the experimental error limit (Fig. 2). With an increase in hydrophobic chain length of the gelator molecule the thermal stability of the gel increased.

### Rheology

The rheology measurement is an important characterization technique to know the mechanical strength of the gels.[38] The strength of gels was evaluated by using elastic modulus (G'), which can estimate the degree of resistance against mechanical disturbance. The tendency of a soft material to flow under stress can be measure by using viscous modulus (G"). The plot of G' and G" versus frequency at constant strain (1%) for the hydrogels (**10-PAM** and **12-PAM** gelators) has been illustrated in Fig. 3a. Both G' and G" were exhibited very little frequency dependence up to 60 Hz. Further, the G' is always greater than G", this shows elastic nature is dominate over viscous nature, which is a characteristic property of the gel.

Further, plots of G' and G" versus imposed strain (%) at constant frequency (1Hz) for the hydrogels of **10-PAM** and **12-PAM** gelators have been depicted in Fig. 3b. Generally, the yield strain value reflects the gel breaking point under the applied force. Gao et al. reported that short alkyl chains gelators exhibits weak hydrophobic interactions, and yields to low mechanical strength to the resultant gel prepared by using short alkyl chain analogue.[39] From Fig. 3b, the "yield strain" values are recorded as 18 and 88 % for **10-PAM** and **12-PAM** gelators respectively. From these results, it can be concluded that the higher chain hydrogel sample has good elastic strength compare to the lower chain hydrogel sample. Overall, the rheological experiment showed the **10-PAM** and **12-PAM** hydrogels are soft viscoelastic solid in nature.

### Morphology of the hydrogels

The non-covalent interactions between gelator molecules are involved in the formation of self assembled morphology of gels. For the preparation of xerogels, the water was removed from the hydrogels by freeze-drying. The morphology studies of the freeze-dried xerogels were carried out by using the field emission scanning electron microscopy. The morphologies for **10-PAM** and **12-PAM** xerogels shows flower bunch and leaf vein structures respectively (Fig. 4).

### XRD

X-ray diffraction experiment was carried out to gain an additional perceptiveness into the self assembled molecular packing structure of the gel formed from **12-PAM**. The XRD of the xerogel gave Bragg reflections at 4.2 nm, 2.1nm, and 1.6 nm (Fig. 5a). The energy minimized structure of **12-PAM** indicated a molecular length of 2.7 nm (Fig. 5b), which is less than from the observed d-spacing value (4.2 nm) from the XRD studies. The d spacing value is slightly lower than twice of the molecular length of the **12-PAM**. This clearly indicates that the gelator molecules were arranged bilayer manner with hydrophobic and hydrophilic interactions which were useful for formation of the gels (Fig. 5c). Similarly, **10-PAM** gelator has d-spacing value of 3.8 nm (Fig. 5a) and molecular length of energy minimized structure is 2.4 nm (Fig. S13).

### Drug incorporation, enzyme-triggered and pH controlled release

The development of appropriate solubilisation and delivery of hydrophobic drug systems are challenging task in pharmaceutical research.[40] Vemula et al. reported hydrophobic drug molecules encapsulation in hydrophobic pockets of the hydrogel and subsequently release of the drug molecules from hydrogel by destroying the gel network structures with lipolase enzyme.[29] Herein, reported a simple

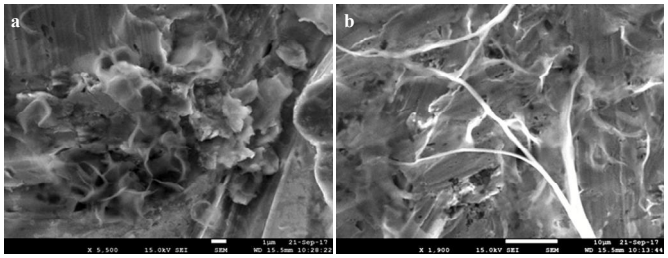


**Fig. 4.** FE-SEM images of the **10-PAM** (a) and **12-PAM** (b) xerogels.

View Article Online
DOI: 10.1039/C8NJ05796F

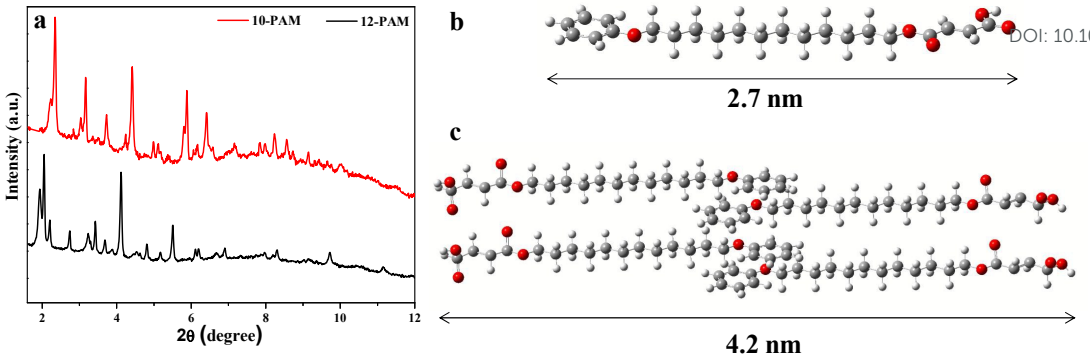


**Fig. 5**. (a) XRD pattern of the **12-PAM** xerogel, (b) Optimized geometries of **12-PAM** gelator molecule, and (c) Schematic representation of the possible molecular packing models for the **12-PAM** gel.

and easily synthesized hydrogelator for the development of single-step enzyme-triggered drug delivery system at the physiological conditions. In the present study, hydrophobic drug curcumin was entrapped in hydrophobic pockets of the hydrogel and the hydrolase enzyme (lypozyme) was used for degradation of hydrogel network structure.

According to previous reports, hydrogels obtained from the chemical modified prodrug gelators and drug loaded thermo-responsive hydrogels are involved in drug delivery process.[41] On the way to prepare the prodrugs, the drug molecules are covalently linked with gelator molecules. This type of gelators may not be easily attainable in all types of drug delivery process. The potential chance of losing original activity of drug molecule will be a major problem while doing the chemical modification of gelator molecule. Herein without chemical modification, a hydrophobic drug molecule was encapsulated in the hydrogel. Subsequently, the drug was released from the gel network structures by the action of enzymatic and pH dependent degradation of gel networks. This is the major advantage over prodrug based hydrogelators.

In the present report curcumin was chosen as the model drug. Curcumin is one of the best-quality hydrophobic drug,[42] extracted from the root of *Curcuma longa*, which shows strong antioxidative, antiinflammatory, and antiseptic activities.[43] Additionally, human immune deficiency virus type 1 (HIV-1) can be inhabited by curcumin.[44] Curcumin is hydrophobic in nature, for which it might be located in hydrophobic pockets of the gel (Fig. 6a). Previously it has been reported that the curcumin is loaded in hydrophobic pockets of the hydrogels.[45–47] The drug encapsulated gel was appeared yellow in colour. The amount of entrapped curcumin in **10-PAM** and **12-PAM** hydrogels was 0.5 and 1% w/v respectively. **12-PAM** showed excellent encapsulation of curcumin as compared to the various gelators reported in the literature.[29,45] Further release studies were performed on the curcumin loaded **12-PAM** gelator, which was having high drug loading capacity.

Tønnesen et al. reported that the solubility of curcumin in water is 3 x $10^{-8}$ M that means in the present study the solubility was enhanced ~9 x $10^{5}$ times in hydrogel.[48] Initially, water (without enzyme) was added on the curcumin loaded hydrogel surface. Significant change in colour of supernatant solution (water) was not noticed even after 24 hours as shown in Fig. 6b. Later, lipozyme solution was added on the preformed drug loaded hydrogel of **12-PAM** (1.3% w/v). Initially, the added solution was colourless and visual changes were observed after some time (Fig. 6c). Vemula et. al. were shown lipase-mediated ester hydrolysis and subsequent gel degradation. Similarly, we anticipated that drug was released from hydrogel by the cleavage of ester bond by lipozyme.[29,45]

The gel degradation and increase in yellow colour intensity of supernatant solution were observed with increase in time. This indicates that upon addition of enzyme solution, encapsulated curcumin has been released into the solution by breaking of the gel networks. UV-absorption spectroscopy was used to evaluate the curcumin release profile in the presence of an enzyme. Aliquots collected at various time intervals showed absorption maxima at 425 nm, which corresponds to the absorption peak of curcumin (Fig. 7).[29,45] The curcumin released from the hydrogel due to gel degradation by enzymatically was confirmed. To further confirm the function of enzyme on hydrogel degradation, a control experiment was performed on the hydrogel without curcumin. As expected, after 24 hours visual changes were not observed in hydrogel (Fig. 6d). In the presence of enzyme, the complete gel degradation was observed after 14 hours as observed in the presence of curcumin (Fig. 6c and e).

The hydrogels are more stable for more than a month at neutral pH, but it was slowly converted from the gel to

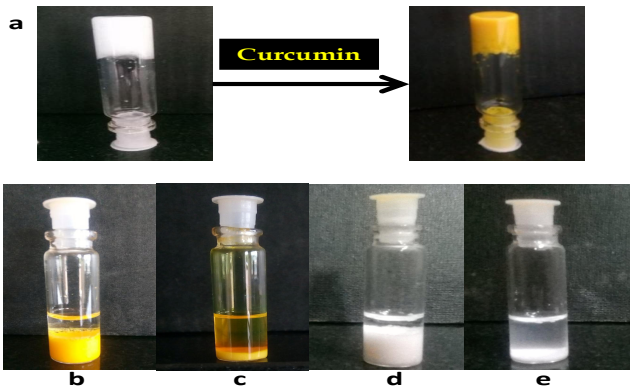


**Fig. 6.** (a) Visual image of curcumin loaded hydrogel, (b-e) Image showing enzymatic hydrogel degradation in absence and presence of curcumin, (b) curcumin entrapped hydrogel in the absence of enzyme, (c) curcumin entrapped hydrogel in presence of enzyme, (d) hydrogel in the absence of enzyme, and (e) hydrogel in presence of enzyme.

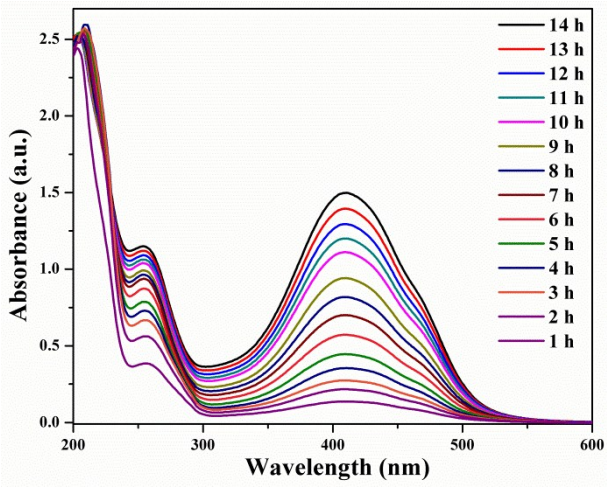


**Fig. 7.** Absorption spectra of curcumin released from degradation of **12-PAM** hydrogel at different time points 1 to 14h (after 14h absorbance did not increase).

solution state at acidic medium (pH = 3.5). The acidity of the medium will increase with adding of buffer solution to the gel sample. As we observed in the preparation of gel, **12-PAM** will form stable gel at pH 8. At pH < 8, it get precipitating and pH > 8, it was forming a clear solution. Similarly, the addition of acid to the **12-PAM** hydrogel decreased the pH of the solution from pH 8, thus by slow degradation of gel. This behaviour clearly shows that, the terminal carboxylic acid groups play vital role in the self-assembly process through formation of hydrogen-bonding network. The pH response on gel could be observed visually by the naked eye. Formulation of hydrophobic drug in hydrogel and subsequent stimuli responsive drug delivery with various external factors are useful in biotechnology processes.[49]

From this information, the pH responsive gel degradation of the **12-PAM** gelator is useful to encapsulate the drug in hydrophobic packets of hydrogels and subsequent release by changing the pH of the medium.[36,50] Drug release from the hydrophobic core of hydrogel in the presence of acidic medium and this process was visually observed Fig. 8a. The kinetic degradation profile of the drug loaded hydrogel was monitored by a kinetic absorption study. The degradation of drug loaded hydrogel can be directly correlated with drug release. The pH responsive cumulative release of curcumin from the curcumin loaded hydrogel was shown in Fig. 8b. From Fig. 8b, the degradation of gel and subsequent release of curcumin was increased with time. The complete degradation gel was attained after 55 minutes.

The schematic representation of curcumin encapsulation and enzyme-mediated release were shown in Fig. 9. The hydrophobic drug, curcumin was trapped into hydrophobic pockets of the hydrogel. Further, addition of lypozyme solution to the hydrogel starts degrading the network structure and subsequent release of curcumin from the gel networks. The gel degradation was happened due to the cleavage of ester bond between phenoxy alkanol and maleic anhydride by lypozyme. It should be noteworthy to mention, enzyme responsive and

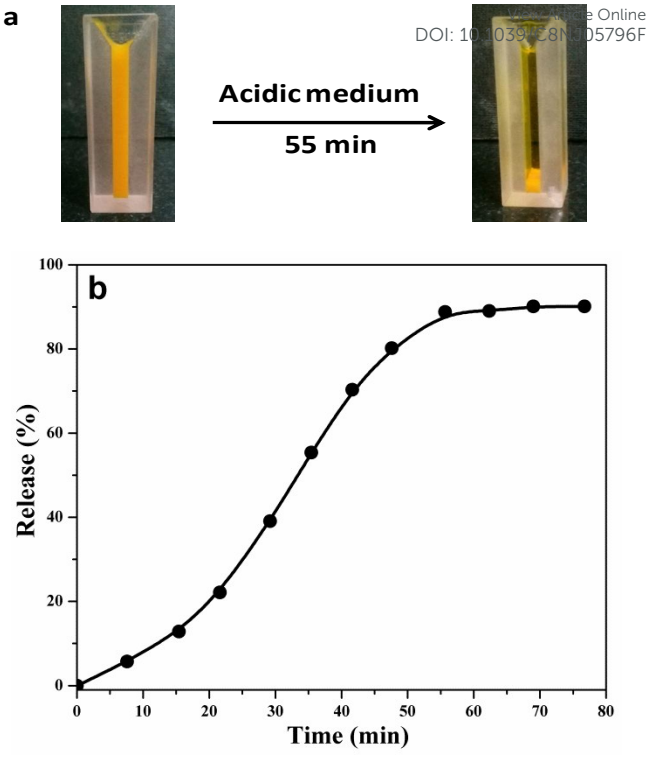


**Fig. 8.** (a) Photographic image of pH responsive curcumin releases from the hydrogel, (b) The pH responsive cumulative release on curcumin from **12-PAM** hydrogel.

pH sensitive drug release behaviours of the hydrogel could plays significant role in pharmaceutical applications.

## Conclusions

In summary, four phenoxy-alkyl maleate based amphiphiles were synthesized using cost effective starting materials and tested for hydrogelation property in phosphate buffer solution at pH 8. **10-PAM** and **12-PAM** gelators were formed stable and thermoreversibility hydrogels. From DSC results we concluded that **12-PAM** shown better thermal stability compared with the **10-PAM**. FE-SEM analysis suggests hierarchical structure such as flower bunch and leaf vein structures for **10-PAM** and **12-PAM** respectively. Mechanical strength of **12-PAM** hydrogel was superior in comparision to the **10-PAM** gel. Encapsulation of curcumin (1%) in the hydrophobic pockets of **12-PAM** hydrogel was achieved. Trapped hydrophobic drug was released from gel network structure by the lipozyme enzyme. Herein, ester bond between phenoxy alkanol and maleic anhydride was hydrolysed by the enzyme. Hydrolysis of gelator molecule leads to gel degradation and subsequent release of curcumin from gel networks. In addition, when the curcumin trapped hydrogel was exposed to acidic pH, the curcumin was efficiently released within 55 min. The curcumin released from the composed hydrogel confirmed by UV-visible spectroscopic studies. Based on the output of this present work, we anticipate that these hydrogels will find applications as the drug carrier agent in the pharmaceutical field.

View Article Online
DOI: 10.1039/C8NJ05796F

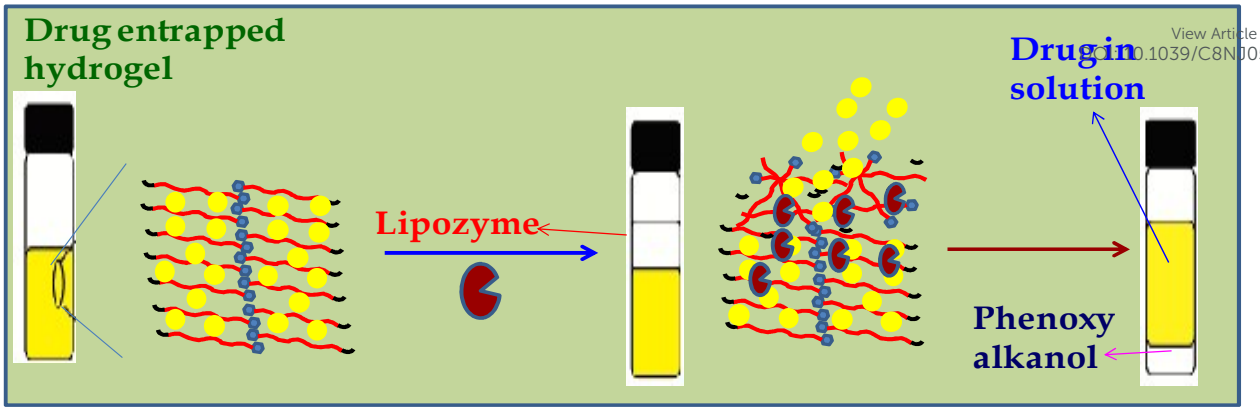


**Fig. 9.** Schematic representations of drug encapsulation and subsequent enzymatic drug release from hydrogel network structure.

## Conflicts of interest

There are no conflicts to declare.

## Acknowledgements

This work was financially supported by the University Grants Commission (UGC), Government of India for providing fellowship. Authors are thankful to Mrs Swarnalatha for her help in carrying out of FE-SEM experiment.

## References

1 P. McNeice, Y. Zhao, J. Wang, G. F. Donnelly and P. C. Marr, *Green Chem.*, 2017, **19**, 4690–4697.
2 C. S. Hawes, A. D. Lynes, K. Byrne, W. Schmitt, G. Ryan, M. E. Möbius and T. Gunnlaugsson, *Chem. Commun.*, 2017, **53**, 5989–5992.
3 Z. Li, Y. Huang, D. Fan, H. Li, S. Liu and L. Wang, *Front. Chem. Sci. Eng.*, 2016, **10**, 552–561.
4 D. Kong, Y. Xia, D. Li and R. Hou, *Supramol. Chem.*, 2017, **29**, 102–110.
5 C.-W. Chu and B. J. Ravoo, *Chem. Commun.*, 2017, **53**, 12450–12453.
6 Y. G. Jia, J. Jin, S. Liu, L. Ren, J. Luo and X. X. Zhu, *Biomacromolecules*, 2018, **19**, 626–632.
7 C. Tsitsilianis, G. Serras, C.-H. Ko, F. Jung, C. M. Papadakis, M. Rikkou-Kalourkoti, C. S. Patrickios, R. Schweins and C. Chassenieux, Macromolecules, 2018, **51**, 2169–2179.
8 Y. Zhang, J. Ji, H. Li, N. Du, S. Song and W. Hou, *Soft Matter*, 2018, **14**, 1789–1798.
9 Z. Li, H. Bai, S. Zhang, W. Wang, P. Ma and W. Dong, *New J. Chem.*, 2018, **42**, 13453–13460.
10 Y. Gao, Y. Li, X. Zhao, J. Hu and Y. Ju, *RSC Adv.*, 2015, **5**, 102097–102100.
11 Zhang, R.; Xue, M.; Yang, J.; Tan, T. *Journal of Applied Polymer Science*, 2012, **125**, 1116-1126.
12 S.-S. Han, H. Y. Yoon, J. Y. Yhee, M. O. Cho, H.-E. Shim, J.-E. Jeong, D.-E. Lee, K. Kim, H. Guim, J. H. Lee, K. M. Huh and S.-W. Kang, *Polym. Chem.*, 2018, **9**, 20–27.
13 H. Liu, C. Wang, C. Li, Y. Qin, Z. Wang, F. Yang, Z. Li and J. Wang, *RSC Adv.*, 2018, **8**, 7533–7549.
14 G. Yang, X. Wan, Z. Gu, X. Zeng and J. Tang, *J. Mater. Chem. B*, 2018, **6**, 1622–1632.
15 K. Bauri, M. Nandi and P. De, *Polym. Chem.*, 2018, **9**, 1257–1287.
16 T. Sun, C. Zhu and J. Xu, *Soft Matter*, 2018, **14**, 921–926.
17 D. Jain, A. Karajic, M. Murawska, B. Goudeau, S. Bichon, S. Gounel, N. Mano, A. Kuhn and P. Barthélémy, *ACS Appl. Mater. Interfaces*, 2017, **9**, 1093–1098.
18 F. Chen, Q. Chen, L. Zhu, Z. Tang, Q. Li, G. Qin, J. Yang, Y. Zhang, B. Ren and J. Zheng, *Chem. Mater.*, 2018, **30**, 1743–1754.
19 T. R. Hoare and D. S. Kohane, *Polymer (Guildf).*, 2008, **49**, 1993–2007.
20 A. S. Puranik, L. P. Pao, V. M. White and N. A. Peppas, *Ind. Eng. Chem. Res.*, 2016, **55**, 10576–10590.
21 D. Gopinath, M. R. Ahmed, K. Gomathi, K. Chitra, P. K. Sehgal and R. Jayakumar, *Biomaterials*, 2004, **25**, 1911–1917.
22 R. K. Maheshwari, A. K. Singh, J. Gaddipati and R. C. Srimal, *Life Sci.*, 2006, **78**, 2081–2087.
23 B. P. Sahu, H. Hazarika, R. Bharadwaj, P. Loying, R. Baishya, S. Dash and M. K. Das, *Expert Opin. Drug Deliv.*, 2016, **13**, 1065–1074.
24 Yallapu, M. M.; Jaggi, M.; Chauhan, S. C. *Drug Discov Today*, 2012, **17**, 71–80.
25 L. Niu, F. Zhu, B. Li, L. Zhao, H. Liang, Y. Yan and H. Tan, *Mater. Chem. Front.*, 2018, **2**, 1529–1538.
26 Y. Chen, Y. Gao, L. P. Da Silva, R. P. Pirraco, M. Ma, L. Yang, R. L. Reis and J. Chen, *Polym. Chem.*, 2018, **9**, 4063–4072.
27 N. Ninan, A. Forget, V. P. Shastri, N. H. Voelcker and A. Blencowe, *ACS Appl. Mater. Interfaces*, 2016, **8**, 28511–28521.
28 J. B. Guilbaud, C. Rochas, A. F. Miller and A. Saiani, *Biomacromolecules*, 2013, **14**, 1403–1411.
29 P. K. Vemula, J. Li and G. John, *J. Am. Chem. Soc.*, 2006, **128**, 8932–8938.
30 M. Zelzer, S. J. Todd, A. R. Hirst, T. O. McDonald and R. V. Ulijn, *Biomater. Sci.*, 2013, **1**, 11–39.
31 J. M. Knipe, F. Chen and N. A. Peppas, *Biomacromolecules*, 2015, **16**, 962–972.
32 S. K. Bajpai and S. Saxena, *J. Appl. Polym. Sci.*, 2004, **92**, 3630–3643.
33 M. Takeda, K. Kondo, S. Sanda, D. Kan, I. K. Borges, I. Suzuki and M. Katahira, *Int. J. Biol. Macromol.*, 2018, **109**, 323–328.
34 B. A. Kumar, S. R. Chowdhury, S. Mishra and R. R. Nayak, *Colloids Surfaces A Physicochem. Eng. Asp.*, 2018, **537**, 310–317.
35 B. A. Kumar and R. R. Nayak, *Soft Mater.*, 2018, **16**, 108–116.
36 K. Lalitha, Y. S. Prasad, C. U. Maheswari, V. Sridharan, G. John and S. Nagarajan, J. Mater. Chem. B, 2015, **3**, 5560–5568.
37 M. J. Frisch, G. Trucks, H. Schlegel, G. Scuseria, M. Robb, J. Cheeseman, G. Scalmani, V. Barone, B. Mennucci and G. Petersson, Gaussian Inc., Wallingford, CT, 2009.
38 L. M. De Leon Rodriguez, Y. Hemar, J. Cornish and M. A. Brimble, *Chem. Soc. Rev.*, 2016, **45**, 4797–4824.
39 Y. Gao, L. Duan, S. Guan, G. Gao, Y. Cheng, X. Ren and Y. Wang, *RSC Adv.*, 2017, **7**, 44673–44679.

View Article Online
DOI: 10.1039/C8NJ05796F

40 T. Miyata, T. Uragami and K. Nakamae, *Adv. Drug Deliv. Rev.*, 2002, **54**, 79–98.
41 K. J. C. van Bommel, M. C. a Stuart, B. L. Feringa and J. van Esch, *Org. Biomol. Chem.*, 2005, **3**, 2917.
42 A. Duvoix, R. Blasius, S. Delhalle, M. Schnekenburger, F. Morceau, E. Henry, M. Dicato and M. Diederich, *Cancer Lett.*, 2005, **223**, 181–190.
43 Hergenhahn, M.; Soto, U.; Weninger, A.; Polack, A.; Hsu, C.H.; Cheng, A.L.; Rösl, F. *Mol. Carcinog.* 2002, ***33***, 137–145.
44 A. Mazumder, K. Raghavan, J. Weinstein, K. W. Kohn and Y. Pommier, *Biochem. Pharmacol.*, 1995, **49**, 1165–1170.
45 P. K. Vemula, G. A. Cruikshank, J. M. Karp and G. John, Biomaterials, 2009, **30**, 383–393.
46 A. V. Divakaran, L. B. Azad, S. S. Surwase, A. Torris A.T. and M. V. Badiger, Chem. Mater., 2016, 28, 2120–2130.
47 X. Li, S. Chen, B. Zhang, M. Li, K. Diao, Z. Zhang, J. Li, Y. Xu, X. Wang and H. Chen, Int. J. Pharm., 2012, **437**, 110–119.
48 H. H. Tønnesen, M. Másson and T. Loftsson, Int. J. Pharm., 2002, **244**, 127–135.
49 P. K. Vemula, N. Wiradharma, J. A. Ankrum, O. R. Miranda, G. John and J. M. Karp, Curr. Opin. Biotechnol., 2013, **24**, 1174–1182.
50 J. Liu, C. Detrembleur, A. Debuigne, M. C. De Pauw-Gillet, S. Mornet, L. Vander Elst, S. Laurent, E. Duguet and C. Jérôme, J. Mater. Chem. B, 2014, **2**, 1009–1023.

View Article Online
DOI: 10.1039/C8NJ05796F



## Table of contents

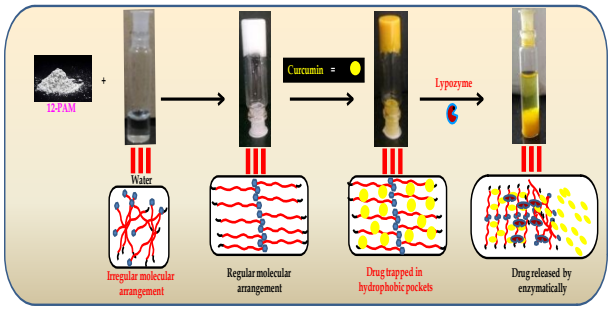


**Text:** Low molecular weight hydrogelators as stimuli responsive drug carrier agent in the pharmaceutical field.